Polymer Journal, Vol. 36, No. 11, pp. 920—926 (2004)

Synthesis and Characterization of Side-Chain Cholesteric Liquid Crystalline Polysiloxanes Containing Diosgeninyl Groups

Jian-She HU, Bao-Yan ZHANG,† Wei PAN, and Wen-Qiang XIAO

Center for Molecular Science and Engineering, Northeastern University, Shenyang 110004, People's Republic of China

(Received June 21, 2004; Accepted August 20, 2004; Published November 15, 2004)

ABSTRACT: New cholesteric liquid crystalline polysiloxanes derived from diosgeninyl groups were synthesized. The chemical structures of the monomers and polymers obtained were confirmed by element analyses, Fourier transform infrared, proton nuclear magnetic resonance and carbon-13 nuclear magnetic resonance spectra. Their mesogenic properties were investigated by polarizing optical microscopy, differential scanning calorimetry, thermogravimetric analysis, and X-ray diffraction measurements. Monomer $\mathbf{M}_1$ exhibited monotropic cholesteric focal-conic texture, and $\mathbf{M}_2$ showed enantiotropic cholesteric phase. Homopolymers showed smectic phase and copolymers showed cholesteric phase. The experimental results demonstrated that the phase behavior and the mesophase temperature ranges of the polymers obtained were affected by the copolymer composition. [DOI 10.1295/polymj.36.920]

KEY WORDS Liquid Crystalline Polymers / Cholesteric Phase / Diosgeninyl Groups /

Side-chain cholesteric liquid crystalline polymers (LCPs) have attract considerable interest mainly due to their unique optical properties, including selective reflection of light, thermochromism and circular dichroism, and advanced applications such as non-linear optical devices, full-color thermal imaging and organic pigment.[1–9] The cholesteric phase is formed by rodlike, chiral molecules responsible for macroscopical alignment of cholesteric domains. Depending to chemical structures, it may be feasible to achieve a macroscopic alignment of cholesteric domains. For comblike polymers, the mesogenic properties of side-chain LCPs mainly depend on the nature of polymer backbone, the type of the mesogen, the length of the flexible spacer, and the nature of terminal groups.[10–13] The polymer backbones of side-chain LCPs are primarily polyacrylates, polymethacrylates and polysiloxanes, however, polyacrylates and polymethacrylates, because of their backbones, show higher glass transition temperatures (T_g) and higher viscosity. For higher mobility of the mesophase and mesogenic properties at moderate temperature, the polysiloxanes' backbone and the flexible spacer are usually chosen and used. Recently, many novel side chain cholesteric LC materials have been reported.[14–23] Therefore, it would be necessary to synthesize various kinds of side-chain cholesteric LCPs to explore their potential applications.

As a very important raw material or intermediate product of steroid hormone, diosgenin is usually used. However, to the best of our knowledge, very little research on LCPs derived from diosgeninyl groups has been reported.[24] In this article, a series of LCPs derived from diosgeninyl 10-undecen-1-ylenate (M_1) and diosgeninyl 4-(10-undecen-1-yloyloxy)benzoate (M_2) were synthesized. The structures and LC properties of the monomers and polymers obtained were characterized with element analyses (EA), Fourier transform infrared (FT IR), proton nuclear magnetic resonance (^{1}H NMR) and carbon-13 nuclear magnetic resonance (^{13}C NMR) spectra, polarizing optical microscopy (POM), differential scanning calorimetry (DSC), thermogravimetric analysis (TGA), and X-ray diffraction (XRD) measurements.

EXPERIMENTAL

Materials

Polymethylhydrosiloxane (PMHS, $\bar{M}_n = 700$–800) was purchased from Jilin Chemical Industry Co. Diosgenin was purchased from Wuhan Ruixin Chemical Co. Hexachloroplatinate(IV) catalyst was obtained from Shenyang Chemical Reagent Co. Toluene used in the hydrosilylation reaction was first refluxed over sodium and then distilled under nitrogen. All other solvents and reagents were purified by standard methods.

Characterization

FT IR spectra were measured on a PerkinElmer spectrum One (B) spectrometer (PerkinElmer, Foster City, CA). The quantitative element analyses (EA) were carried out by using a Elementar Vario EL III (Elementar, Germany). ^{1}H NMR spectra (300 MHz) and ^{13}C NMR (75.4 MHz) spectra were obtained with a Varian Gemini 300 spectrometer (Varian Associates, Palo Alto, CA, U.S.A.). Optical rotations were obtained on a PerkinElmer 341 polarimeter. Phase

†To whom correspondence should be addressed (E-mail: baoyanzhang@hotmail.com).

transition temperatures and thermodynamic parameters were determined by using a Netzsch DSC 204 (Netzsch, Wittelsbacherstr, Germany) equipped with a liquid nitrogen cooling system. The heating and cooling rates were 10 °C/min. The thermal stability of the polymers under atmosphere was measured with a Netzsch TGA 209C thermogravimetric analyzer. A Leica DMRX (Leica, Wetzlar, Germany) polarizing optical microscope equipped with a Linkam THMSE-600 (Linkam, Surrey, U.K.) hot stage was used to observe phase transition temperatures and analyze LC properties for the monomers and polymers through observation of optical textures. XRD measurements were performed with a nickel-filtered Cu Kα (λ = 1.542 Å) radiation with a DMAX-3A Rigaku (Rigaku, Tokyo, Japan) powder diffractometer.

Synthesis of the Monomers

The synthetic route to the olefinic monomers is shown in Scheme 1. 4-(10-undecen-1-yloyloxy)benzoic acid **1** was prepared according to the reported literature.[25]

Diosgeninyl 10-Undecen-1-ylenate (M_1)

Undecenyl acid chloride (20.3 g, 0.1 mol) was added dropwise to a cold solution of diosgenin (41.4 g, 0.1 mol) in tetrahydrofuran (150 mL) and triethylamine (14 mL). After refluxing for 10 h, the reaction mixture was poured into much water. The crude product was obtained by filtration, and washed with dilute hydrochloric acid and water. White crystals were obtained by recrystallization with ethanol. Yield = 62%; mp = 99 °C; $[\alpha]^{28}_{D}$ −64.7° (c = 0.789, toluene).

IR (KBr, cm^{-1}): 3074 (=C–H); 2926, 2851 (–CH_3, –CH_2–); 1727 (C=O); 1632 (C=C).

Elem. Anal. Calcd for $C_{38}H_{60}O_4$: C, 78.57%; H, 10.41%. Found: C, 78.35%; H, 10.52%.

^{1}H NMR ($CDCl_3$, TMS) δ ppm: 0.78–2.26 [m, 52H, –(CH_2)$_8$– and diosgeninyl–*H*]; 3.32–3.54 (m, 3H, >C*H*O– and –OCH_2– in diosgeninyl); 4.35–4.61 (m, 1H, –COOC*H*<); 4.92 (d, 2H, CH_2=CH–); 5.37 (d, 1H, =C*H*– in diosgeninyl), 5.80 (m, 1H, =C*H*–).

^{13}C NMR ($CDCl_3$, TMS, δ, ppm): 6.2, 20.1, 20.5, 20.8 (methyl–C); 20.6, 25.3, 25.9, 26.9, 29.4, 29.9, 30.1, 30.5, 32.0, 32.6, 32.8, 33.2, 33.9, 34.0, 39.6, 70.1 (methylene–C); 29.7, 29.9, 38.4, 39.8, 42.7, 47.8, 68.2, 76.4 (tertiary C); 34.5, 38.8, 111.1 (quaternary C); 114.7 (CH_2=); 139.8 (=CH–); 123.2 (=CH– in diosgeninyl); 149.3 (>C= in diosgeninyl); 171.5 (C=O).

Diosgeninyl 4-(10-Undecen-1-yloyloxy)benzoate (M_2)

4-Undecenyloyloxybenzoyl chloride (16.2 g, 0.05 mol) was added dropwise to a cold solution of diosgenin (20.7 g, 0.05 mol) in chloroform (100 mL) and triethylamine (7 mL). The reaction mixture was refluxed for 13 h. The excess solvent and precipitate were removed, crude product was obtained by adding ethanol to filtrate, and recrystallized from ethanol. White solid were obtained. Yield = 59%; mp = 116 °C; $[\alpha]^{28}_{D}$ −33.9° (c = 0.769, toluene).

IR (KBr, cm^{-1}): 3071 (=C–H); 2927, 2854 (–CH_3, –CH_2–); 1763, 1712 (C=O); 1641 (C=C); 1604, 1457 (Ar–).

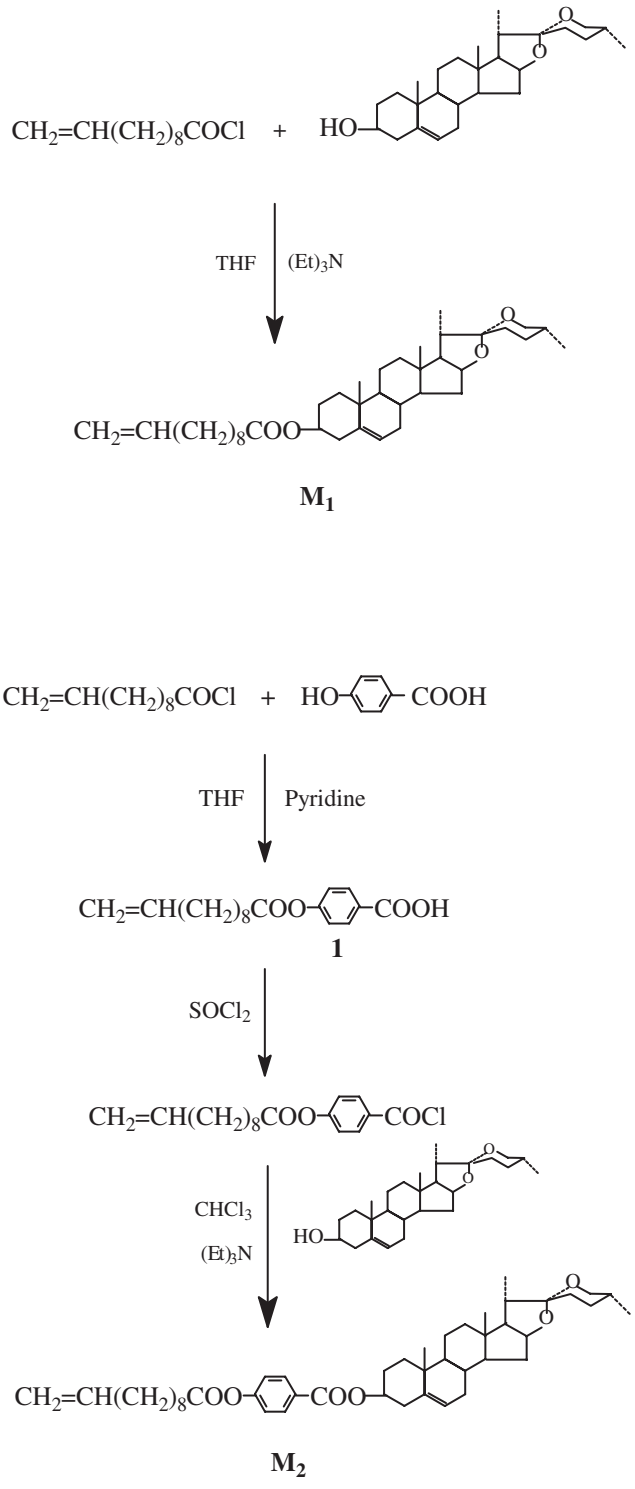

Scheme 1. Synthesis of LC monomers.

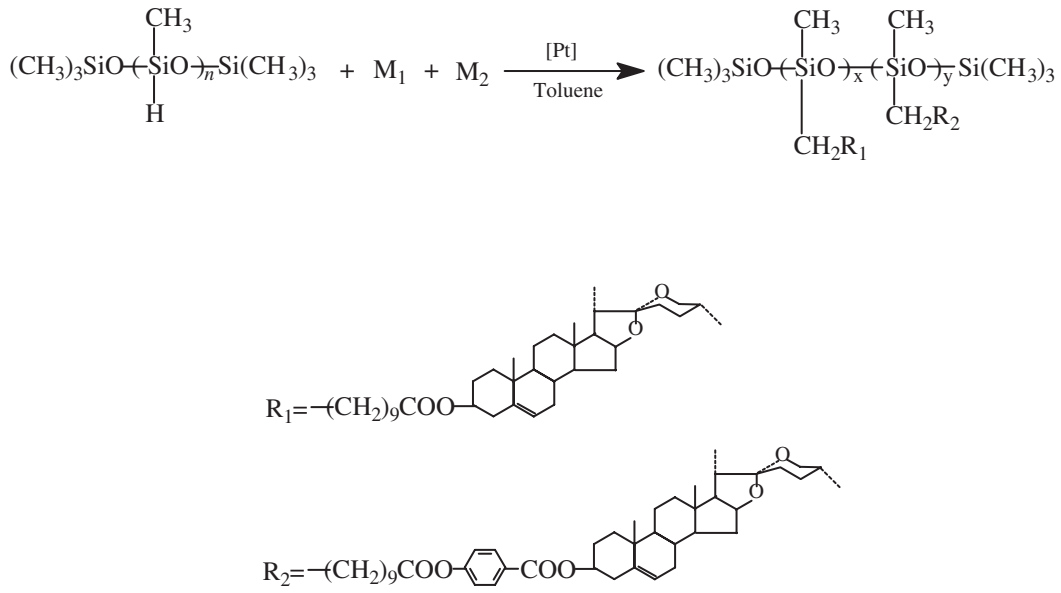

Scheme 2. Synthesis of LC polysiloxanes.

Elem. Anal. Calcd for $C_{45}H_{64}O_6$: C, 77.10%; H, 9.20%. Found: C, 76.91%; H, 9.28%.

^{1}H NMR ($CDCl_3$, TMS) δ ppm: 0.78–2.56 [m, 52H, –(CH_2)$_8$– and diosgeninyl–*H*]; 3.33–3.51 (m, 3H, >C*H*O– and –OCH_2– in diosgeninyl); 4.40 (m, 1H, –ArCOOC*H*<); 4.87 (d, 2H, CH_2=CH–); 5.42 (d, 1H, =C*H*– in diosgeninyl), 5.82 (m, 1H, =C*H*–); 7.13–8.08 (m, 4H, Ar–*H*).

^{13}C NMR ($CDCl_3$, TMS, δ, ppm): 6.6, 15.6, 20.1, 20.4 (methyl–C); 21.3, 23.8, 25.3, 27.5, 30.1, 30.3, 30.6, 30.9, 31.7, 32.5, 32.9, 33.1, 33.2, 33.5, 34.1, 38.9, 68.1 (methylene–C); 28.8, 30.2, 35.5, 41.1, 43.5, 47.4, 67.2, 76.8 (tertiary C in diosgeninyl); 120.8, 129.6 (aromatic tertiary C); 35.3, 39.7, 112.3 (quaternary C in diosgeninyl); 127.7, 158.1 (aromatic quaternary C); 113.2 (CH_2=); 141.5 (=CH–); 122.4 (=CH– in diosgeninyl); 148.1 (>C= in diosgeninyl); 166.3, 170.4 (C=O).

Synthesis of Polymers

The synthesis of the polysiloxanes $\mathbf{P}_1$–$\mathbf{P}_7$ is shown in Scheme 2. $\mathbf{P}_1$–$\mathbf{P}_7$ were synthesized by equivalent methods. The monomers $\mathbf{M}_1$, $\mathbf{M}_2$, and PMHS, fed in Table I, were dissolved in toluene. The reaction mixture was heated to 65 °C under nitrogen, and then 2 mL of THF solution of hexachloroplatinate(IV) catalyst (5 mg/mL) was injected with a syringe. The hydrosilylation reaction was completed within 30 h as indicated by IR. The polymers were obtained by precipitation with methanol, and then dried in vacuum.

IR (KBr): 2927–2853 (–CH_3, –CH_2–); 1766, 1736, 1718 (C=O); 1606, 1510 (Ar–); 1300–1000 cm^{-1} (Si–O–Si, C–Si and C–O–C).

Table I. Polymerization and solubility

Polymer	Feed (mmol)		M_2[a] (mol%)	Yield (%)	Solubility[b]	
	$\mathbf{M}_1$	$\mathbf{M}_2$			Toluene	THF
$\mathbf{P}_1$	7.00	0.00	0	93	+	+
$\mathbf{P}_2$	6.00	1.00	14.3	90	+	+
$\mathbf{P}_3$	5.00	2.00	28.6	92	+	+
$\mathbf{P}_4$	4.00	3.00	42.9	89	+	+
$\mathbf{P}_5$	3.00	4.00	57.1	91	+	+
$\mathbf{P}_6$	2.00	5.00	71.4	90	+	+
$\mathbf{P}_7$	0.00	7.00	100	92	+	+

[a]Molar fraction of M_2 based on (M_1 + M_2). [b]+soluble.

RESULTS AND DISCUSSION

Synthesis

The monomers and polymers obtained were synthesized according to Schemes 1 and 2. $\mathbf{M}_1$ and $\mathbf{M}_2$ were prepared by the corresponding acid chloride reacted with diosgenin in chloroform in present of pyridine. Structures of $\mathbf{M}_1$ and $\mathbf{M}_2$ were characterized by IR, ^{1}H and ^{13}C NMR spectrum. ^{1}H NMR spectra of $\mathbf{M}_1$ and $\mathbf{M}_2$ were shown in Figure 1a and 1b. IR spectra of $\mathbf{M}_2$ confirmed the presence of characteristic bands at 1763 1712, 1604, and 1457 cm^{-1} attributed to ester C=O and aromatic stretching band. ^{1}H NMR spectra of $\mathbf{M}_2$ showed multiplet at 8.08–7.13, 5.82–4.87, and 2.56–0.78 ppm corresponding to aromatic protons, olefinic protons, and methyl and methylene protons, respectively. The spectra of $\mathbf{M}_1$ and $\mathbf{M}_2$ suggest that the purity is high and this was confirmed by EA.

The polymers were prepared by hydrosilylation reaction. IR spectra of the polymers showed the complete disappearance of Si–H stretching band at

(a)

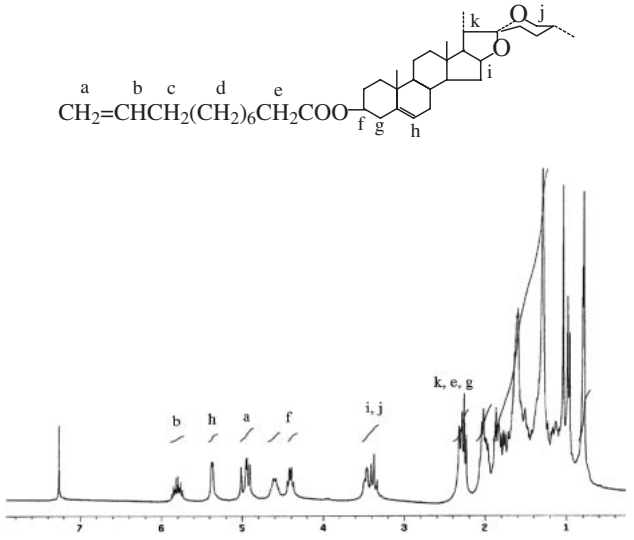

$\mathbf{M_1}$

(b)

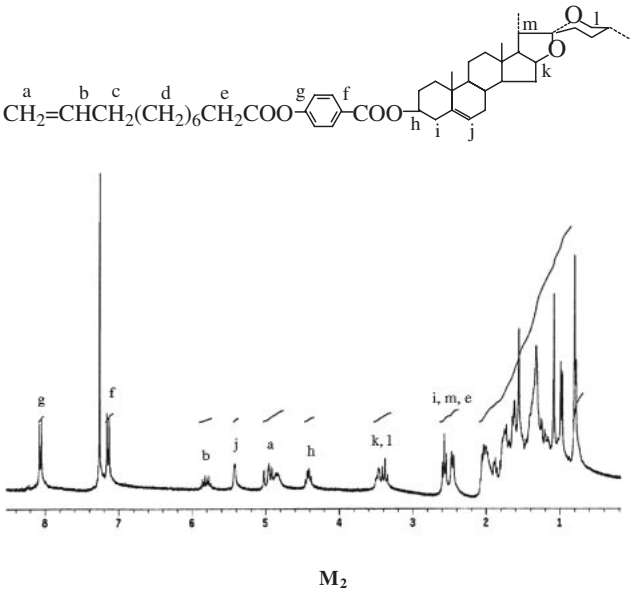

$\mathbf{M_2}$

Figure 1. ^{1}H NMR spectra of monomers: (a) $\mathbf{M}_1$; (b) $\mathbf{M}_2$.

2166 cm^{-1}. Characteristic Si–O–Si stretching bands appeared at 1300–1000 cm^{-1}. In addition, the absorption bands of ester C=O and aromatic still existed. The polymerization, yields and solubility of the polymers are summarized in Table I. All polymers were a powder, and were soluble in toluene, xylene, and tetrahydrofuran.

Optical Textures

Cholesteric materials at zero field exhibit two optically contrasting stable states: planar (including oily-streak and Grandjean) texture and focal-conic texture. When cholesteric phase is in the planar texture, the helical axis is perpendicular to the cell surface, the material reflects colored light; when cholesteric phase is in the focal-conic texture, the helical axis is more or less parallel to the cell surface, the material is forward-scattering and does not appear selective light reflection.

The optical textures of the monomers and polymers are observed by POM with hot stage under nitrogen atmosphere. POM observation showed that $\mathbf{M}_1$ showed monotropic phase and $\mathbf{M}_2$ displayed enantiotropic cholesteric phase. When $\mathbf{M}_1$ was heated to 98 °C, the sample melt and no LC phase appeared. When the isotropic state was cooled to 86 °C, the cholesteric focal-conic texture appeared, and crystallized at 66 °C. When $\mathbf{M}_2$ was heated to 114 °C, the sample began to melt, heating continued to 138 °C, a cholesteric oily-streak texture appeared and the reflection color changed from red, green to blue with increasing temperature from 138 to 149 °C. The texture disappeared at 161 °C. Cooling isotropic to LC state, the focal-conic texture and spiral texture appeared. Optical textures of $\mathbf{M}_1$ and $\mathbf{M}_2$ are shown in Figure 2a and 2b.

The homopolymers $\mathbf{P}_1$ and $\mathbf{P}_7$ showed the smectic fan-shaped textures, and the expected cholesteric tex-

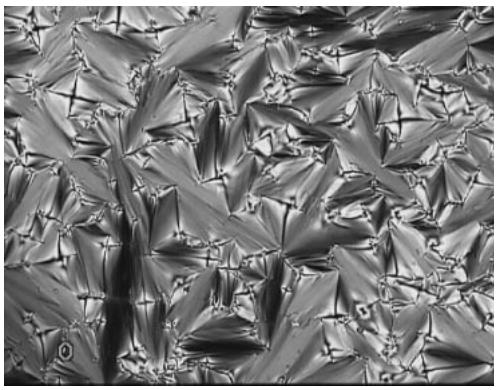

(a)

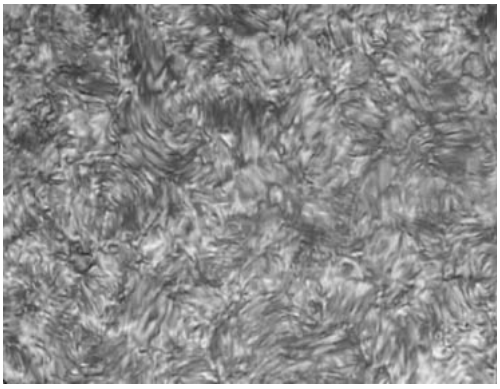

(b)

Figure 2. Optical textures of monomers (200×): (a) focal-conic texture of $\mathbf{M}_1$ on cooling to 71.2 °C; (b) spiral texture of $\mathbf{M}_2$ on cooling to 73.6 °C.

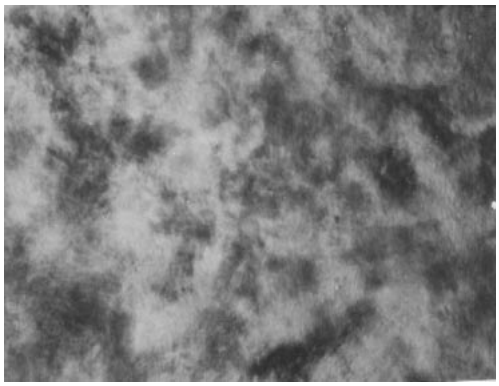

Figure 3. Optical textures of $\mathbf{P}_4$ at 182.3 °C (200×).

Table II. Phase transition temperatures of monomers

Monomers	Transition temperature[a,b] in °C (Corresponding enthalpy changes in J g^{-1}) Heating / Cooling
$\mathbf{M}_1$	K99.1(45.0)I / I83.0(1.4)Ch
$\mathbf{M}_2$	K116.3(25.3)Ch156.9(0.5)I / I152.1(0.5)Ch68.2(22.9)K

[a]K = solid, Ch = cholesteric, I = isotropic. [b]Peak temperatures were taken as the phase transition temperature.

ture did not occur because of the polymeric chains hinder the formation of helical supermolecular structure of the mesogens and the mesogenic moieties are ordered in a smectic orientation with their centers of gravity in planes. The copolymers $\mathbf{P}_2$–$\mathbf{P}_6$ exhibited cholesteric Grandjean texture, but selective reflection properties were not observed. Photomicrograph of $\mathbf{P}_4$ as an example is shown in Figure 3.

Thermal Properties

The phase transition temperatures and corresponding enthalpy changes of monomers $\mathbf{M}_1$, $\mathbf{M}_2$ and polymers $\mathbf{P}_1$–$\mathbf{P}_7$, obtained on the second heating and the first cooling scan, are summarized in Tables II and III. Representative DSC traces of monomer and polymers are presented in Figures 4 and 5. All phase transitions were reversible and did not change on repeated heating and cooling cycles. The phase transition temperatures determined by DSC were consistent with POM.

DSC heating thermogram of $\mathbf{M}_2$ contained two endotherms of the phase, which represented a melting transition at 116.3 °C and a cholesteric–isotropic phase transition at 156.9 °C. On cooling scans of $\mathbf{M}_1$ and $\mathbf{M}_2$, an isotropic–cholesteric phase transition appeared at 83.0 and 152.1 °C, respectively.

DSC thermogram of $\mathbf{P}_1$–$\mathbf{P}_5$ showed a glass transition at low temperature and a LC–isotropic phase transition at high temperature. However, the DSC curve of $\mathbf{P}_6$ and $\mathbf{P}_7$ only showed a glass transition; no obvious LC–isotropic phase transition was seen, but POM results showed $\mathbf{P}_6$ and $\mathbf{P}_7$ displayed mesomorphic prop-

Table III. Thermal properties of polymers

Polymer	T_g (°C)	T_i (°C)	ΔH_i (J g^{-1})	ΔT[b]	T_{onset}[c] (°C)	T_d[d] (°C)
$\mathbf{P}_1$	43.2	183.7	1.21	140.5	213.7	339.0
$\mathbf{P}_2$	53.5	208.1	3.56	154.6	249.4	338.2
$\mathbf{P}_3$	58.5	213.6	2.91	155.1	242.5	332.9
$\mathbf{P}_4$	57.4	220.7	1.79	163.3	236.0	328.8
$\mathbf{P}_5$	64.1	223.3	2.35	159.2	233.3	323.6
$\mathbf{P}_6$	64.6	245[a]	—	180.4	231.3	328.7
$\mathbf{P}_7$	66.5	294[a]	—	227.5	251.9	326.1

[a]Detection with POM at 10 °C/min; [b]Mesophase temperature ranges (T_i–T_g); [c]Temperature for initial thermal decomposition; [d]Temperature at which 5% weight loss occurred.

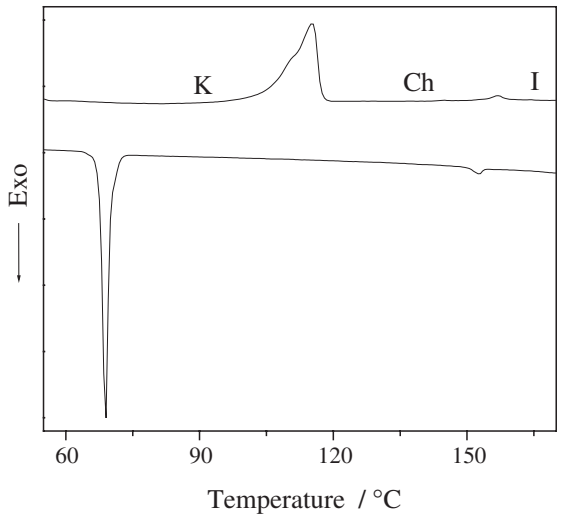

Figure 4. DSC thermograms of monomer $\mathbf{M}_2$.

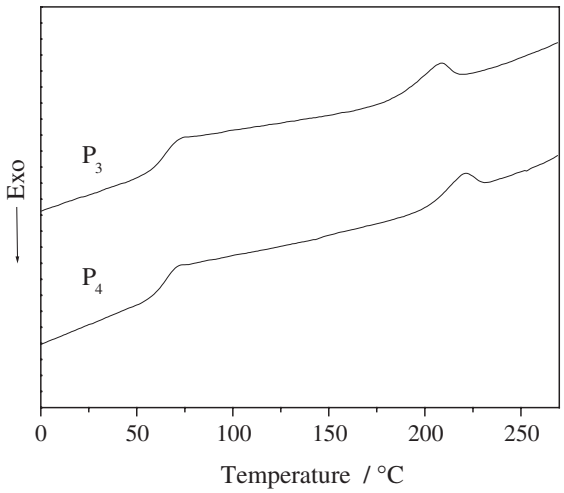

Figure 5. DSC thermograms of polymers.

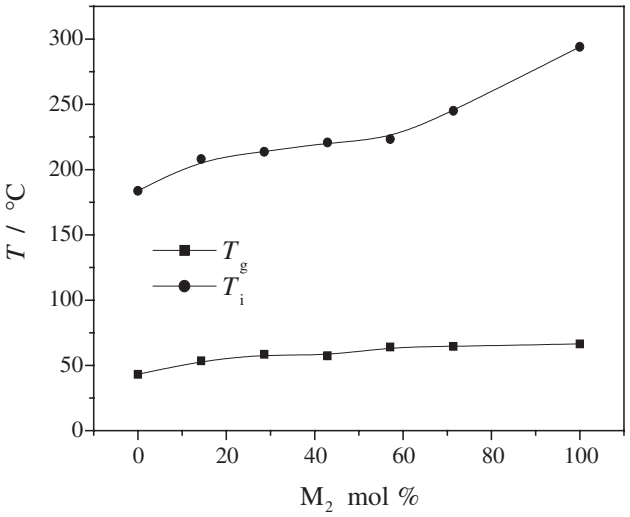

Figure 6. Effect of $\mathbf{M}_2$ content on the phase transition temperatures of the polymers.

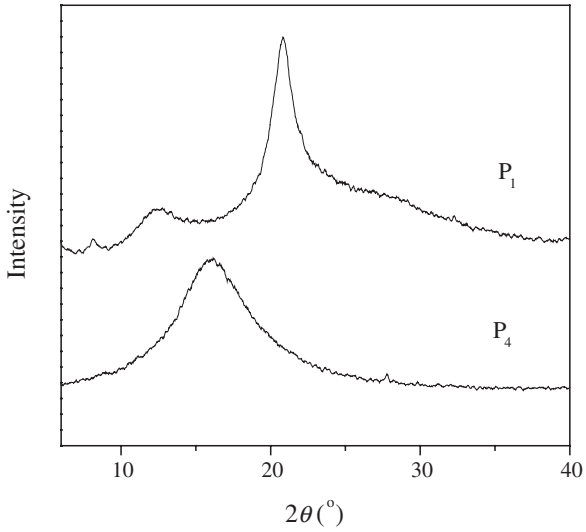

Figure 7. X-ray diffraction patterns of quenched samples.

erties. The reason for which is that the initial thermal decomposition temperatures (T_{onset}) are lower than the clearing temperature (T_i). Figure 6 shows the influence of the copolymer composition on the phase behavior of the polymers. With increasing the concentration of $\mathbf{M}_2$ units in the polymers, T_g and T_i increased.

It is well-known that T_g is an important parameter in connection with structures and properties. For side-chain LCPs, T_g is influenced by the nature of the polymer backbone, the rigidity of the mesogenic groups, the length of the flexible spacer, and the copolymer composition. As shown in Table III, T_g increased from 43.2 °C of $\mathbf{P}_1$ to 66.5 °C of $\mathbf{P}_7$ when the concentration of $\mathbf{M}_2$ increased from 0 to 100 mol % for the following reasons: the rigidity of the mesogenic side groups increased with increasing the concentration of $\mathbf{M}_2$. Similar to T_g, T_i increased from 183.7 °C of $\mathbf{P}_1$ to 294 °C of $\mathbf{P}_7$. Moreover, the mesophase temperature ranges (ΔT) also increased because of T_i increased more than T_g. This indicates that the mesomorphic properties of the polymers are strongly influenced by the $\mathbf{M}_2$ concentration.

The thermal stability of the polymers is usually detected with TGA. The carbon, hydrogen and oxygen atom in the polymers have been completely combusted when heated to 600 °C. TGA results of the polymers are shown in Table III. TGA results showed that the temperatures at which 5% weight loss occurred (T_d) were greater than 320 °C for $\mathbf{P}_1$–$\mathbf{P}_7$, this demonstrates that the synthesized polymers have a high thermal stability.

X-ray Diffraction

In general, a sharp and strong peak at low angle ($1^\circ < 2\theta < 4^\circ$) in small-angle X-ray scattering (SAXS) curves and a strong broad peak associated with lateral packing at about $2\theta = 20^\circ$ can be observed in wide-angle X-ray diffraction (WAXD) curves for a smectic structure; no peak appears in SAXS curves and a broad peak occurred at t $2\theta =$ 16–18° for a cholesteric structure. Figure 7 shows representative XRD curves of quenched samples. A strong small-angle reflection associated with the smectic layers was observed at $2\theta = 2.3$ and 2.5°, and 20.5 and 21.1°, corresponding to d-spacing of $d =$ 38.4 and 35.3 Å, and 4.3 and 4.2 Å for $\mathbf{P}_1$ and $\mathbf{P}_7$. A strong small-angle reflection was not observed and a broad peak appeared at about $2\theta = 16^\circ$ for $\mathbf{P}_2$–$\mathbf{P}_6$, corresponding to d-spacing of $d = 5.5$ Å. Therefore, the LC phase structure was confirmed by POM and XRD results.

CONCLUSIONS

In this study, two cholesteric monomers and a series of LCPs derived from diosgeninyl groups were synthesized and characterized. Monomers $\mathbf{M}_1$ showed monotropic cholesteric phase and $\mathbf{M}_2$ showed enantiotropic cholesteric phase. Homopolymers $\mathbf{P}_1$ and $\mathbf{P}_7$ showed smectic phase, and copolymers $\mathbf{P}_2$–$\mathbf{P}_6$ showed cholesteric phase. All of the obtained polymers exhibited wider mesophase temperature ranges and high thermal stability. For $\mathbf{P}_1$–$\mathbf{P}_7$, T_g and T_i increased with increasing the concentration of $\mathbf{M}_2$ units.

Acknowledgment. The authors are grateful to *National Natural Science Fundamental Committee of China, HI-Tech Research and development program (863) of China, Science and Technology Research Major Project of Ministry of Education of China, and Science and Technology Bureau of Shenyang* for financial support of this work.

REFERENCES

1. D. G. McDonell, in "Thermotropic Liquid Crystals, 2nd ed," G. W. Gray, Ed., John Wiley & Sons, Inc., New York, N. Y., 1987, p 120.
2. S. V. Belayev, M. I. Schadt, J. Funfschiling, N. V. Malimoneko, and K. Schmitt, *Jpn. J. Appl. Phys.*, **29**, 634 (1990).
3. D. J. Broer, J. Lub, and G. N. Mol, *Nature*, **378**, 467 (1995).
4. T. J. Bunning and F. H. Kreuzer, *Trends Polym. Sci.*, **3**, 318 (1995).
5. D. K. Yang, J. L. West, L. C. Chien, and J. W. Doane, *J. Appl. Phys.*, **76**, 1331 (1994).
6. H. R. Kricheldorf, S. J. Sun, and C. P. Chen, *J. Polym. Sci., Part A: Polym. Chem.*, **35**, 1611 (1997).
7. P. M. Peter, *Nature*, **391**, 745 (1998).
8. B. Sapich, J. Stumpe, and H. R. Kricheldorf, *Macromolecules*, **31**, 1016 (1998).
9. S. J. Sun, L. C. Liao, and T. C. Chang, *J. Polym. Sci., Part A: Polym. Chem.*, **38**, 1852 (2000).
10. P. Le Barney, J. C. Dubois, C. Friedrich, and C. Noel, *Polym. Bull.*, **15**, 341 (1986).
11. C. S. Hsu and V. Percec, *J. Polym. Sci., Part A: Polym. Chem.*, **27**, 453 (1989).
12. C. J. Hsiech, S. H. Wu, G. H. Hsiue, and C. S. Hsu, *J. Polym. Sci. Part A: Polym. Chem.*, **32**, 1077 (1994).
13. Y. H. Wu, Y. H. Lu, and C. S. Hsu, *J. Macromol. Sci., Pure Appl. Chem.*, **32**, 1471 (1995).
14. A. Stohr and P. Strohriegl, *Macromol. Chem. Phys.*, **199**, 751 (1998).
15. I. Dierking, L. L. Kosbar, and G. A. Held, *Liq. Cryst.*, **24**, 387 (1998).
16. T. Pfeuffer and P. Strohriegl, *Macromol. Chem. Phys.*, **200**, 2480 (1999).
17. M. A. Espinosa, V. Cadiz, and M. Galia, *J. Polym. Sci., Part A: Polym. Chem.*, **39**, 2847 (2001).
18. H. Finkelmann, S. T. Kim, A. Munoz, and B. Taheri, *Adv. Mater.*, **13**, 1069 (2001).
19. S. T. Kim and H. Finkelmann, *Macromol. Rapid Commun.*, **22**, 429 (2001).
20. J. S. Hu, B. Y. Zhang, K. Sun, and Q. Y. Li, *Liq. Cryst.*, **30**, 1267 (2003).
21. B. Y. Zhang, J. S. Hu, Y. G. Jia, and B. G. Du, *Macromol. Chem. Phys.*, **204**, 2123 (2003).
22. J. S. Hu, B. Y. Zhang, Y. G. Jia, and S. Chen, *Macromolecules*, **36**, 9060 (2003).
23. B. Y. Zhang, J. S. Hu, Y. Wang, and J. H. Qian, *Polym. J.*, **35**, 476 (2003).
24. N. W. Adams, J. S. Bradshaw, J. M. Bayona, K. E. Markides, and M. L. Lee, *Mol. Cryst. Liq. Cryst.*, **147**, 43 (1987).
25. J. S. Hu, B. Y. Zhang, L. M. Liu, and F. B. Meng, *J. Appl. Polym. Sci.*, **89**, 3944 (2003).